Proceedings of the 17th World Congress
The International Federation of Automatic Control
Seoul, Korea, July 6-11, 2008

Multi-Rate Path-Following Control for Unmanned Air Vehicles ⋆

D. Antunes * **C. Silvestre** * **R. Cunha** *

* *Instituto Superior Tecnico, Institute for Systems and Robotics*
Av. Rovisco Pais, 1, 1049-001 Lisboa, Portugal
{*dantunes,cjs,rita*}*@isr.ist.utl.pt*

Abstract: A methodology is provided to tackle the path-following integrated guidance and control problem for unmanned air vehicles with measured outputs available at different rates. The path-following problem is addressed by defining a suitable non-linear path dependent error space to express the vehicle's nonlinear dynamics. The main novelty of the method is to explicitly take into account the different temporal characteristics of the onboard sensor suite in the controller design and implementation. The proposed controller solution relies on a linear parameter varying structure that naturally exploits these multi-rate characteristics of the system outputs to obtain the desired properties for the resulting integrated guidance and control system. Due to the periodic time-varying characteristics of the multi-rate mechanism, the controller synthesis is dealt with under the scope of linear periodic systems theory. The effectiveness of the path-following methodology is accessed in simulation for low altitude terrain-following maneuvers of a small-scale helicopter using a full dynamic model of the vehicle.

1. INTRODUCTION

This paper presents a path following control solution for unmanned air vehicles (UAVs) that naturally takes into account the multi-rate characteristics of the onboard sensor suite. This feature is of paramount importance in UAVs applications where the linear position measurements are typically available at a lower rate than that of the remaining variables, as is the case when using the Global Positioning System (GPS).

In the field of motion control for autonomous vehicles, path-following has proven to be an efficient alternative to trajectory tracking. While in the trajectory tracking problem the vehicle is expected to follow a reference defined in terms of space and time-coordinates, in the path-following problem the vehicle is required to converge and to follow a path without temporal restrictions. In this way, path-following approaches usually exhibit enhanced performance when compared to trajectory tracking (Aguiar and Hespanha (2007)), with smoother convergence to the path and less demand on the control effort. In Cunha and Silvestre (2005) a solution was presented for the path-following problem for unmanned air vehicles that relies on the definition of an error space to accurately model the vehicle's nonlinear equations. By taking into account both the kinematics and dynamics this approach provides an integrated guidance and control solution to the problem of motion control for UAVs.

Multi-rate control theory has received considerable attention in the last few decades (see, for example Colaneri and Nicolao (1995), Lall and Dullerud (2001) and the references therein). If we assume that the sensor sampling and actuators updating rates are related by rational numbers, a multi-rate system can be modeled as a periodic system (Lall and Dullerud (2001)). In applications for autonomous vehicles the multi-rate nature of the sensor suite can either be taken into account in the navigation system (Vasconcelos et al. (2004)) or directly in the controller. This latter approach is followed in Antunes et al. (2007) where a gain-scheduling control methodology is proposed for the control of multi-rate nonlinear systems, which eliminates the need to feedforward the values of the state variables and inputs at trimming. Gain-scheduling control is a powerful technique extensively used in aerospace applications that exploits the advantages of linear systems controller design to synthesize a nonlinear compensator, which typically has a linear parameter varying (LPV) structure (Rugh and Shamma (2000)).

In this paper the path-following problem is addressed by defining a suitable non-linear path dependent error space to express the vehicle's nonlinear dynamics (see Cunha and Silvestre (2005)). The proposed controller design methodology relies on a linear parameter varying structure with integral action that takes into account the multi-rate characteristics of the sensors and actuators. Based on this structure a gain-scheduling controller design and implementation procedure is followed (Rugh and Shamma (2000)), where the multi-rate linear controller synthesis problem is addressed within the scope of the H_2 control theory for linear discrete time periodic systems.

The proposed technique is applied to the design of a multi-rate integrated guidance and control system for a small-scale helicopter, which is evaluated in simulation for a low

⋆ This work was partially supported by Fundação para a Ciência e a Tecnologia (ISR/IST pluriannual funding) through the POS Conhecimento Program that includes FEDER funds and by the PTDC/EEA-ACR/72853/2006 HELICIM project. The work of D. Antunes was supported by a PhD Student Scholarship, SFRH/BD-/24632/2005, from the Portuguese FCT POCTI programme.

altitude terrain following maneuver. The reference path considered is composed by the concatenation of straight lines and results from applying a terrain reconstruction technique to Laser Range Scanner measurements (Paulino et al. (2006)).

The remainder of the paper is organized as follows. We briefly introduce the helicopter model in Section 2. The path-following problem formulation is presented in Section 3 and the controller design methodology for nonlinear multi-rate system is described in Section 4. Section 5 focuses on the controller design and implementation procedure. Finally, simulation results are presented in Section 6 and the concluding remarks in Section 7.

The notation is fairly standard. The space of n-dimensional continuous-time signals, $x(t) : \mathbb{R}^+ \mapsto \mathbb{R}^n$, will be denoted by $\mathcal{L}(\mathbb{R}^+, \mathbb{R}^n)$ or simply by $\mathcal{L}(\mathbb{R}^+)$ and the space of n-dimensional discrete-time signals, $x_k : \mathbb{Z}^+ \mapsto \mathbb{R}^n$, will be denoted by $l(\mathbb{Z}^+, \mathbb{R}^n)$ or simply by $l(\mathbb{Z}^+)$. The notation $\mathrm{diag}([a_1 \ a_2 \ \dots \ a_n])$ indicates a block diagonal matrix where the entries a_i can be either scalar or matrices. Whenever the matrices dimensions are clear, identity and zero matrices are denoted by I and 0. Otherwise the dimensions are explicit indicated as in I_3, $0_{3\times 2}$. A vector of n ones is denoted by $1_n = [1 \ 1 \ \dots \ 1]^T$. Further notation will be introduced when necessary.

2. HELICOPTER DYNAMIC MODEL

This section summarizes the helicopter dynamic model. For a comprehensive coverage the reader is referred to Cunha and Silvestre and Cunha (2002) where a full nonlinear dynamic model of a small-scale helicopter is derived from first principles.

Let $({}^I p_B, \ {}^I_B R) \in SE(3) := \mathbb{R}^3 \times SO(3)$ denote the configuration of the body frame attached to the vehicle's center of mass $\{B\}$ with respect to the inertial frame $\{I\}$, where ${}^I_B R = {}^B_I R^T = R_Z(\psi_B) R_Y(\theta_B) R_X(\phi_B)$ is a rotation matrix parameterized by the Z-Y-X Euler angles $\lambda = [\phi_B \ \theta_B \ \psi_B]^T$, $\theta_B \in \,]-\pi/2, \pi/2[$, $\phi_B, \psi_B \in \mathbb{R}$. In addition, let $v = [u_B \ v_B \ w_B]^T$ and $\omega = [p_B \ q_B \ r_B]^T$, denote the linear and angular body velocities, respectively, where $v = {}^B_I R \, {}^I\dot{p}_B$, $\omega = {}^B_I R \, {}^I\omega_B$, and ${}^I\omega_B$ is the angular velocity of $\{B\}$ with respect to $\{I\}$. The helicopter dynamics can then be described by using the conventional six degree of freedom rigid body equations of motion

$$\begin{cases} \dot{v} = \dfrac{1}{m}[f(v, \omega, u) + {}^B_I R\,[0 \ 0 \ g]^T] - w \times v \\ \dot{\omega} = I^{-1} n(v, \omega, u) - I^{-1}(w \times Iw) \\ {}^I\dot{p}_B = {}^I_B R \, v \\ \dot{\lambda} = Q(\phi_B, \theta_B)\, \omega \end{cases}, \qquad (1)$$

where m is the vehicle mass, and I is the tensor of inertia about the frame $\{B\}$. The actuation $u = [\theta_0 \ \theta_{1s} \ \theta_{1c} \ \theta_{0t}]$ comprises the main rotor collective input θ_0, the main rotor cyclic inputs, θ_{1s} and θ_{1c}, and the tail rotor collective input θ_{0t}. The force and moment vectors can be decomposed as $f = f_{mr} + f_{tr} + f_{fus} + f_{tp} + f_{fn}$ and $n = n_{mr} + n_{tr} + n_{fus} + n_{tp} + n_{fn}$, respectively, where the subscripts mr, tr, fus, tp and fn stand for main rotor, tail rotor, fuselage, horizontal tail plane and vertical tail, respectively. The simulation model includes the rigid body, main rotor flapping, and Bell-Hiller stabilizing bar dynamics, which are not presented here for the sake of brevity but can be found in Cunha and Silvestre.

3. PATH-FOLLOWING FORMULATION

The integrated guidance and control strategy proposed in Cunha and Silvestre (2005) for the path-following problem consists in defining a path-dependent transformation, which is applied to the vehicle's dynamic and kinematic model to express it in a convenient error space. The problem of steering the unmanned vehicle along a predefined path with a given velocity profile, is then reduced to that of regulating the error variables to zero. In order to present this transformation, we first introduce the frames $\{T\}$ and $\{C\}$, depicted in Fig. 1, and a collection of references associated to these frames. These elements can be briefly described as follows (see Cunha and Silvestre (2005) for further details and derivations):

Frame $\{T\}$

There is an almost exact correspondence between $\{T\}$ and the standard Serret-Frenet frame. The x axis, x_T, is aligned with the tangent vector to the path, so that the linear velocity reference in this frame is given by

$$v_r = V_r \, [1 \ 0 \ 0]^T$$

where V_r is the desired linear speed. The angular velocity reference, also expressed in $\{T\}$, can be written as

$$\omega_r = V_r \, [\tau \ 0 \ \kappa]^T$$

where τ is the torsion and κ the curvature, which characterize each point on the path. The frame $\{T\}$ moves along the path attached to the point on the path closest to the vehicle, meaning that the position error can be defined as the two-dimensional vector $d_t = [d_y \ d_z]^T \in \mathbb{R}^2$ that satisfies

$$\begin{bmatrix} 0 \\ d_t \end{bmatrix} = {}^T_I R({}^I p_B - {}^I p_T),$$

where ${}^I p_T$ is the position of $\{T\}$ with respect to $\{I\}$. It is also useful to consider the Z-Y-X Euler angles $\lambda_T = [\phi_T \ \theta_T \ \psi_T]^T$, which describe the orientation of $\{T\}$, and the linear speed V_T, which is related to the vehicle's velocity by

$$V_T = \frac{1}{1 - \kappa \, d_y} \, [1 \ 0 \ 0] \ {}^T_B R \, v.$$

Frame $\{C\}$

The need to define $\{C\}$ arises from the fact that while following a path, the vehicle may take different orientations or even rotate with respect to the path. The reference of orientation for the vehicle is given by the Z-Y-X Euler angles $\lambda_C = [\phi_C \ \theta_C \ \psi_C]^T$, $\theta_C \in \,]-\pi/2, \pi/2[$, $\phi_C, \psi_C \in \mathbb{R}$. The angular velocity of $\{C\}$ with respect to $\{T\}$ expressed in $\{T\}$ is denoted by ${}^T\omega_C$. The origin of $\{C\}$ coincides with that of $\{T\}$.

Given the definitions of $\{T\}$ and $\{C\}$, the error state vector $x_e \in \mathbb{R}^{11}$ can be defined as

$$x_e = \begin{bmatrix} v_e \\ \omega_e \\ d_t \\ \lambda_e \end{bmatrix} = \begin{bmatrix} v - {}^B_T R \, v_r \\ \omega - {}^B_T R\,(\omega_r + {}^T\omega_C) \\ \Pi_{yz} \, {}^T_I R({}^I p_B - {}^I p_T) \\ \lambda - \lambda_C \end{bmatrix}, \ \Pi_{yz} = \begin{bmatrix} 0 & 1 & 0 \\ 0 & 0 & 1 \end{bmatrix}. \qquad (2)$$

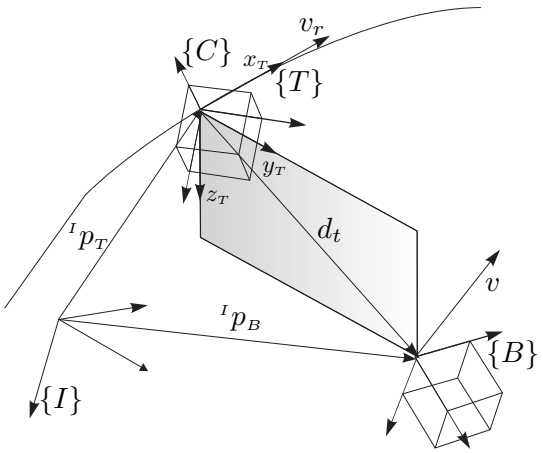

Fig. 1. Coordinate frames: inertial $\{I\}$, body $\{B\}$, tangent $\{T\}$, and desired body frame $\{C\}$

It is easy to see that the vehicle follows the path with the desired velocity profile and orientation if and only if $x_e = 0$ (regulation problem).

If we restrict the set of possible paths to the set of trimming paths, the error dynamics can be parameterized by a set of variables that only depend on the trimming path. A trimming path corresponds to a curve that the vehicle can follow while satisfying the trimming conditions, which is equivalent to having $\dot{v} = 0$, $\dot{\omega} = 0$, and $\dot{u} = 0$ in (1). It is well known that for a vehicle with dynamics described by (1), the set of trimming trajectories comprises all z-aligned helices ($\dot{\kappa} = 0$, $\dot{\tau} = 0$, $\lambda_T = [0\ \theta_T\ \psi_T]^T$, and $\dot{\lambda}_T = \text{sign}(\kappa) V_T \sqrt{\kappa^2 + \tau^2}\,[0\ 0\ 1]^T$), followed at constant speed ($\dot{V}_T = 0$) and constant orientation with respect to the path (${}^T\omega_C = 0$) (Silvestre et al. (2002)). Consider the following variables: the linear speed reference V_r, the flight path angle θ_T, the yaw orientation of the vehicle with respect to the path $\psi_{ct} = \psi_c - \psi_t$ and the yaw rate $\dot{\psi}_r = V_r \sqrt{\kappa^2 + \tau^2}$. As discussed in Cunha and Silvestre (2005), for the case of helicopters this set of variables

$$\xi = (V_r,\ \dot{\psi}_r,\ \theta_T,\ \psi_{ct}) \tag{3}$$

adequately parameterizes the vehicle's equilibrium points corresponding to trimming paths. The error dynamics defined with respect to these operating points can be written as

$$\mathcal{P}(\xi) := \begin{cases} \dot{x}_e = f_e(x_e, u, \xi) \\ y_e = h_e(x_e, \xi) \end{cases}, \tag{4}$$

and is such that $f_e(0, u_\xi, \xi) = 0$ and $h_e(0, \xi) = 0$. The output y_e is chosen in such a way that at steady state the condition $y_e = 0$ implies $x_e = 0$, therefore characterizing an equilibrium point. It can be shown that the output given by

$$y_e = \begin{bmatrix} v_e + {}^B_T R \begin{bmatrix} 0 \\ d_t \end{bmatrix} \\ \psi_e \end{bmatrix} \in \mathbb{R}^4 \tag{5}$$

verifies this condition. By applying integral action to (5), we can guarantee that y_e (and consequently x_e) goes to zero at steady-state.

Recalling that ξ is a constant parameter vector, the linearization of $\mathcal{P}(\xi)$ about ($x_e = 0$, $u = u_\xi$) results in a family of linear time-invariant systems of the form

$$\mathcal{P}_l(\xi) = \begin{cases} \dot{x}_e = A_e(\xi) x_e + B_e(\xi) u_\delta \\ y_e = C_e(\xi) x_e \end{cases}, \tag{6}$$

where $u_\delta = u - u_\xi$, $A_e(\xi) = \dfrac{\partial f_e}{\partial x_e}(0, u_\xi, \xi)$, $B_e(\xi) = \dfrac{\partial f_e}{\partial u}(0, u_\xi, \xi)$, and $C_e(\xi) = \dfrac{\partial h_e}{\partial x_e}(0, \xi)$.

4. NONLINEAR MULTI-RATE CONTROLLER DESIGN

In this section we summarize the gain-scheduling methodology for nonlinear multi-rate systems presented in Antunes et al. (2007), which will be applied to the multi-rate path-following control problem.

4.1 Problem Setup

Consider the nonlinear system

$$G := \begin{cases} \dot{x}(t) = f(x(t), u(t), w(t)) \\ y(t) = h(x(t), w(t)) \end{cases} \tag{7}$$

where $x(t) \in \mathbb{R}^n$ is the state, $u(t) \in \mathbb{R}^m$ is the control input, and the vector $w(t) \in \mathbb{R}^{n_w}$ contains references $r(t)$ and possibly other exogenous inputs. The vector $y(t) \in \mathbb{R}^p$ can be decomposed as $y(t) = [y_m(t)^T\ \ y_r(t)^T]^T = [h_m(x(t), w(t))^T\ \ h_r(x(t), w(t))^T]^T$ where $y_m(t) \in \mathbb{R}^{n_{y_m}}$ is a vector of measured outputs available for feedback and $y_r(t) \in \mathbb{R}^{n_{y_r}}$ is a vector of tracking outputs, which we assume to have the same dimensions as the control input, $n_{y_r} = m$. This vector is required to track the reference $r(t)$ with zero steady state error, i.e. the error vector defined as $e(t) := y_r(t) - r(t)$ must satisfy $e(t) = 0$ at steady-state. Some of the components of $y_r(t)$ may be included in $y_m(t)$ as well.

Linearization family

We assume that there exists a unique family of equilibrium points for G of the form

$$\Sigma := \{(x_0, u_0, w_0) : f(x_0, u_0, w_0) = 0,\ y_{r0} = h_r(x_0, w_0) = r_0\}$$

which can be parameterized by a vector $\alpha_0 \in \Xi \subset \mathbb{R}^s$, such that

$$\Sigma = \{(x_0, u_0, w_0) = a(\alpha_0), \alpha_0 \in \Xi\} \tag{8}$$

where a is a continuously differentiable function. We further assume that there exists a continuously differentiable function v such that $\alpha_0 = v(y_0, w_0)$. Applying the function v to the measured values of y and w, we obtain the variable

$$\alpha = v(y, w), \tag{9}$$

which is usually referred to as the scheduling variable.

Linearizing the system G about the equilibrium manifold Σ parameterized by α_0 yields the family of linear systems

$$G_l(\alpha_0) := \begin{bmatrix} \dot{x}_\delta(t) \\ y_\delta(t) \end{bmatrix} = \begin{bmatrix} A(\alpha_0) & B_1(\alpha_0) & B_2(\alpha_0) \\ C_2(\alpha_0) & D_{21}(\alpha_0) & 0 \end{bmatrix} \begin{bmatrix} x_\delta(t) \\ w_\delta(t) \\ u_\delta(t) \end{bmatrix} \tag{10}$$

where, e.g. $A(\alpha_0) = \frac{\partial f}{\partial x}(a(\alpha_0))$ and $x_\delta(t) = x(t) - x_0$.

Multi-rate sensors and actuators

We consider that the sample and hold devices that interface the discrete-time controller and the continuous-time plant operate at different rates. The actuators updating

and sensor sampling times do not have to be equally spaced but the periodicities of the updating and sampling mechanisms are assumed to be rationally related. Let t_s denote the greatest common divisor of these periods and consider a set of h-periodic matrices $\Gamma_k = \Gamma_{k+h}$, $\Omega_k = \Omega_{k+h}$ taking the form: $\Gamma_k = \text{diag}(g_1(k), ..., g_p(k))$, where $g_i(k) = 1$ if output i is sampled at time $t_k = kt_s$ and $g_i(k) = 0$ otherwise; $\Omega_k := \text{diag}(r_1(k), ..., r_m(k))$, where $r_j(k) = 1$ if input j is updated at time $t_k = kt_s$ and $r_j(k) = 0$ otherwise. Then the multi-rate input and output mechanisms, denoted by S_{mr} and H_{mr}, respectively, can be modeled as

$$\begin{aligned} S_{mr}&:\mathcal{L}(\mathbb{R}^+) \mapsto l(\mathbb{Z}^+) \\ &\quad y_k = \begin{bmatrix} y_{mk} \\ y_{rk} \end{bmatrix} = \begin{bmatrix} \Gamma_{mk} & 0 \\ 0 & \Gamma_{rk} \end{bmatrix} \begin{bmatrix} y_m(t_k) \\ y_r(t_k) \end{bmatrix} = \Gamma_k y(t_k) \\ H_{mr}&:l(\mathbb{Z}^+) \mapsto \mathcal{L}(\mathbb{R}^+) \\ &\quad \xi_{k+1} = (I - \Omega_k)\xi_k + \Omega_k u_k \ \ , \ \xi_0 = 0 \\ &\quad \tilde{u}_k = (I - \Omega_k)\xi_k + \Omega_k u_k \\ &\quad u(t) = \tilde{u}_k \qquad t \in [t_k, t_{k+1}[\end{aligned} \tag{11}$$

We also introduce the error variable $e_k = y_{rk} - r_k$, where $r_k = \Gamma_{rk} r(t_k)$.

4.2 Multi-rate controller design and implementation

Consider the linearized system (10) with multi-rate interface (11) which can be written as the series connection $S_{mr}G_lH_{mr}$. Suppose that given a fixed α_0 we design a linear controller for this multi-rate system that takes the form depicted in Fig. 2. In the figure C_I and C_D correspond to discrete time linear periodic integrators and differentiators, respectively, that can be written as

$$C_I = \begin{cases} x^I_{k+1} = x^I_k + \Omega_k u^I_k \\ y^I_k = x^I_k + \Omega_k u^I_k \end{cases} \tag{12}$$

$$C_D = \begin{cases} x^D_{k+1} = (I - \Gamma_{mk})x^D_k + \Gamma_{mk} u^D_k \\ y^D_k = -\Gamma_{mk} x^D_k + \Gamma_{mk} u^D_k \end{cases} \tag{13}$$

These two systems are introduced is such a way that the controller C_K operates in a differential manner, that is, it takes in the plant's output differential values and provides differential values to be integrated into the actuation signals. The importance of this structure for gain-scheduling control will be clarified shortly.

Consider the system G_a shown in Fig. 2, which is given by the series connection of C_I, $S_{mr}G_lH_{mr}$ and C_D, i.e. $G_a = C_D S_{mr} G_l H_{mr} C_I$. As proved in Antunes et al. (2007), this augmented system G_a preserves the detectability and stabilizability properties of the original system G_l, under mild assumptions. Hence, there exists a stabilizing controller C_K, which is in general periodically time-varying. Furthermore, due to integral action and given that C_K stabilizes the closed-loop system, the structure achieves zero steady-sate error for y_r. Suppose the equations for C_K are given by

$$C_K(\alpha_0) = \left\{ \begin{bmatrix} x^K_{\delta k+1} \\ y^K_{\delta k} \end{bmatrix} = \begin{bmatrix} A^K_k(\alpha_0) & B^K_{1k}(\alpha_0) & B^K_{2k}(\alpha_0) \\ C^K_k(\alpha_0) & D^K_{1k}(\alpha_0) & D^K_{2k}(\alpha_0) \end{bmatrix} \begin{bmatrix} x^K_{\delta k} \\ y^D_k \\ e_k \end{bmatrix} \right.$$

and that we have designed a parameter-dependent family of controllers of the form $C_I C_K(\alpha_0) C_D$.

Consider then the following implementation for the nonlinear gain-scheduled controller, taking the form of a linear parameter varying (LPV) controller and obtained by replacing the time-frozen parameter α_0 with the scheduling variable α_k.

$$K = \left\{ \begin{array}{l} \begin{bmatrix} x^K_{k+1} \\ y^K_k \end{bmatrix} = \begin{bmatrix} A^K_k(\alpha_k) & B^K_{1k}(\alpha_k) & B^K_{2k}(\alpha_k) \\ C^K_k(\alpha_k) & D^K_{1k}(\alpha_k) & D^K_{2k}(\alpha_k) \end{bmatrix} \begin{bmatrix} x^K_k \\ y^D_k \\ e_k \end{bmatrix} \\ \begin{bmatrix} x^D_{k+1} \\ y^D_k \end{bmatrix} = \begin{bmatrix} I - \Gamma_{mk} & \Gamma_{mk} \\ -\Gamma_{mk} & \Gamma_{mk} \end{bmatrix} \begin{bmatrix} x^D_k \\ y_{mk} \end{bmatrix} \\ \begin{bmatrix} x^I_{k+1} \\ u_k \end{bmatrix} = \begin{bmatrix} I & \Omega_k \\ I & \Omega_k \end{bmatrix} \begin{bmatrix} x^I_k \\ y^K_k \end{bmatrix} \\ \alpha_k = v(\tilde{y}_k, w_k) \\ \begin{bmatrix} x^Y_{k+1} \\ \tilde{y}_k \end{bmatrix} = \begin{bmatrix} I - \Gamma_k & \Gamma_k \\ I - \Gamma_k & \Gamma_k \end{bmatrix} \begin{bmatrix} x^Y_k \\ y_k \end{bmatrix} \qquad \text{(14.A)} \end{array} \right. \tag{14}$$

The scheduling variable α_k is computed on-line from the plant outputs and exogenous variables. The system described by (14.A) is used to perform a hold operation on the output y_k so that the scheduling variable α_k is computed, at each iteration, according to the last sampled value of the output. The exogenous vector is assumed to be available at each sampling instant, so that $w_k = w(t_k)$.

Since the proposed controller operates in a differential manner, we can show that it verifies the following the linearization property: At each equilibrium point parameterized by α_0, the gain-scheduled controller K linearizes to the designed controller $C_I C_K(\alpha_0) C_D$. See Rugh and Shamma (2000) for the importance of such property and for examples of incorrect implementations where this property is not verified. The controller structure is inspired in the velocity implementation (Kaminer et al. (1995)) - a technique devised to guarantee that the referred linearization property holds for continuous gain-scheduled controllers, which also operates in a differential manner.

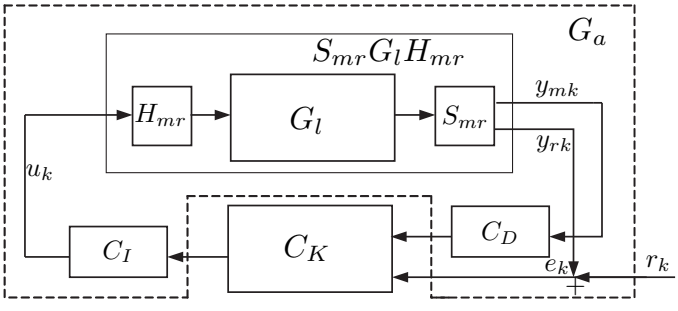

Fig. 2. Regulator structure for non-square systems

5. MULTI-RATE CONTROLLER DESIGN AND IMPLEMENTATION

We assume that the state variables of the vehicle (1) are all available at a rate of 50 Hz except for the components of the linear position, which are assumed to be updated at the lower rate of 2.5 Hz. The actuation update rate is also set to 50 Hz, therefore yielding $h = 20$ and $t_s = 0.02$. In accordance with Section 4.1 and assuming that the nonlinear plant is given by (4), we consider the error output $y_r = y_e$ and define the measured output $y_m = x_e$. The set of matrices Ω_k and Γ_k are determined by

$$\Omega_k = I_4, \quad \Gamma_{mk} = \begin{cases} I_{11} & k = 0 \\ \text{diag}([1_3 \;\; 1_3 \;\; 0_2 \;\; 1_3]) & \text{otherwise} \end{cases},$$
$$\Gamma_{rk} = \begin{cases} I_4 & k = 0 \\ \text{diag}([0_3 \;\; 1]) & \text{otherwise} \end{cases}, \; k = 0, .., h-1. \quad (15)$$

Making use of the controller structure presented in Section 4, a family of linear controllers is designed for the parameterized family of models described by (6) with the multi-rate characteristics just described, using a standard method of gain-scheduling theory. This method comprises the following steps: *i)* obtain a finite set of parameter values from the discretization of the continuous parameter space, *ii)* synthesize a linear controller for each linear plant (6), obtained from the linearization of the nonlinear plant for each value of the scheduling parameter, *iii)* interpolate the coefficients of the linear controllers to obtain a continuously parameter-varying controller. We detail each of these steps in the remainder of this section.

5.1 Discretization of the parameter space

The set of parameters that characterize a trimming path, which corresponds to an equilibrium point for the vehicle's dynamic equation, is given by (3). In this paper, we restrict the set of trimming trajectories considered for terrain-following maneuvers to straight-lines ($\dot{\psi}_r = 0$), with constant linear speed V_r and vehicle's yaw angle aligned with the path ($\psi_{ct} = 0$). The parameter space is then reduced to $\alpha_0 = \theta_T$. Moreover if we assume that $\phi_B = 0$ and $\theta_B = 0$ at trimming and consider the variable

$$\alpha = \arctan(-\frac{w_B}{u_B})$$

we can show that at equilibrium $\alpha = \alpha_0$ (Paulino et al. (2006)), and therefore α conforms with the general description of scheduling variable given in Section 4.1.

The selected set of values for this parameter, $\{\bar{\alpha}_{0i}\}$ is given by

$$\bar{\alpha}_0 = [\text{-}50 \;\; \text{-}40 \;\; \text{-}30 \;\; \text{-}20 \;\; \text{-}10 \;\; 0 \;\; 10 \;\; 20 \;\; 30 \;\; 40 \;\; 50] \frac{\pi}{180} \;\; \text{rad},$$

which means that the conditions under which the vehicle is expected to operate include following straight lines in trimmed flight, with a flight path angle ranging between -50 and 50 degrees.

5.2 Linear controller synthesis

For linear controller synthesis, the standard LQG solution for periodic systems presented in detail in Colaneri and Nicolao (1995) was used to synthesize a controller $C_K(\bar{\alpha}_{0i})$ for each parameter value $\bar{\alpha}_{0i}$. The augmented system $G_a = C_D G_l C_I$ seen by the controller is obtained from (6) and (15). Notice that G_a has $n_{y_m} + n_{y_r} = 11 + 4 = 15$ outputs and $n + m + n_{y_r} = 11 + 4 + 11 = 26$ state variables, which determine the dimensions of C_K. The weights defining the LQG problem were adjusted to yield good transient error responses and smooth actuation for the closed-loop system.

5.3 Interpolation

The resulting finite set of synthesized controller coefficients, for example $\{A_k^K(\alpha_{0i})\}$, were interpolated using least squares yielding a continuously parameter dependent controller $C_I C_K(\alpha_0) C_D$, where the describing matrices are quadratically parameter dependent, for example

$$A_k^K(\alpha_0) = A_k^{K1} + \alpha_0 A_k^{K2} + \alpha_0^2 A_k^{K3}$$
$$B_{1k}^K(\alpha_0) = B_{1k}^{K1} + \alpha_0 B_{1k}^{K2} + \alpha_0^2 B_{1k}^{K3}.$$

The disadvantage of this technique is that there is no guarantee that, even for fixed parameter values, the controller obtained by interpolation stabilizes the closed loop system. This analysis was made a posteriori, verifying that for a dense grid of fixed values of α_0 the closed loop system is stable.

Having designed the continuously parameter varying controller $C_I C_K(\alpha_0) C_D$, the final gain-scheduled controller K takes the form (14), which, as noted earlier, eliminates the need to feedforward the trimming values for the state variables and inputs. Another interesting feature of the methodology is that the implementation of anti-windup schemes is straightforward due to the fact that integral action is provided at the plant's input.

6. RESULTS

The simulation results presented in this section were obtained using the non-linear dynamic model SimModHeli, parameterized for the Vario X-Treme model-scale helicopter (Cunha and Silvestre). The helicopter is required to perform a low altitude terrain-following task, by describing the path shown in Figure (3) with constant linear speed $V_r = 1.5$ m/s. The reference path may result from a terrain following reconstruction algorithm (see Paulino et al. (2006)) and is divided in the four following segments: *i)* a level flight segment along the x axis, *ii)* a climbing ramp with a flight path angle of $\theta_T = 0.5236$ rad, *iii)* a level flight segment along the x axis, and finally *iv)* a descending ramp with a flight path angle of $\theta_T = -0.2618$ rad. Figure (4) shows the time evolution of the errors $v_e = [u_e \, v_e \, w_e]^T$, $\omega_e = [p_e \, q_e \, r_e]^T$, d_t, and $\lambda_e = [\theta_e \, \phi_e \, \psi_e]^T$, actuation, and multi-rate velocity and position signals. From the figure, we can conclude that the helicopter with the gain-scheduling multi-rate controller efficiently performs the desired task. Notice that after each transition, the helicopter quickly converges to the reference path corresponding to zero-steady state errors. Furthermore the actuation is kept within the limits of operation, exhibiting a smooth behavior.

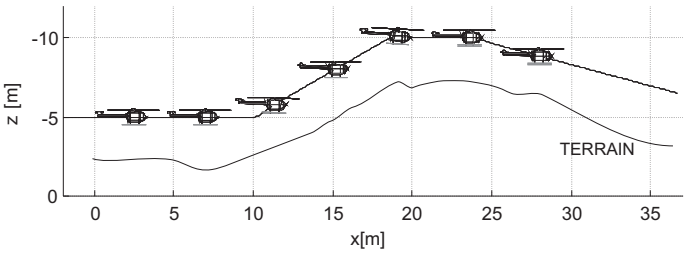

Fig. 3. Helicopter performing a low altitude terrain-following maneuver.

To finalize, for the linear controller synthesis characterized by $\alpha_0 = 0$, Table 1 shows the loss of performance in terms of the values of the closed-loop $\mathcal{H}_2$ norms while changing the rate of the linear position measurement and keeping

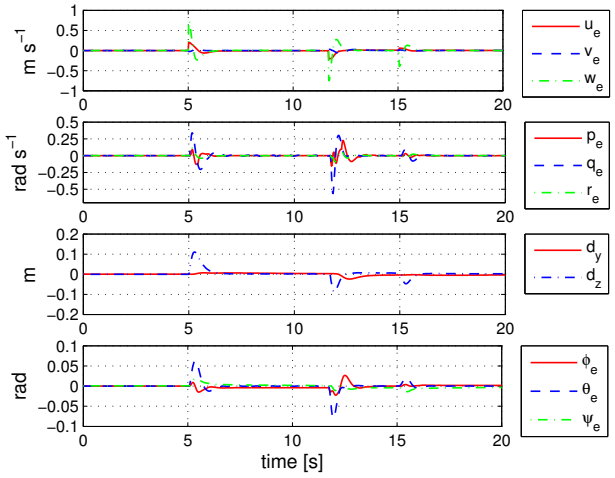

(a) Errors

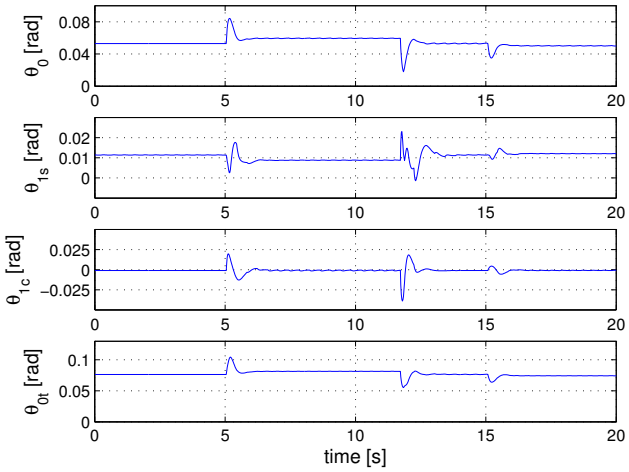

(b) Actuation

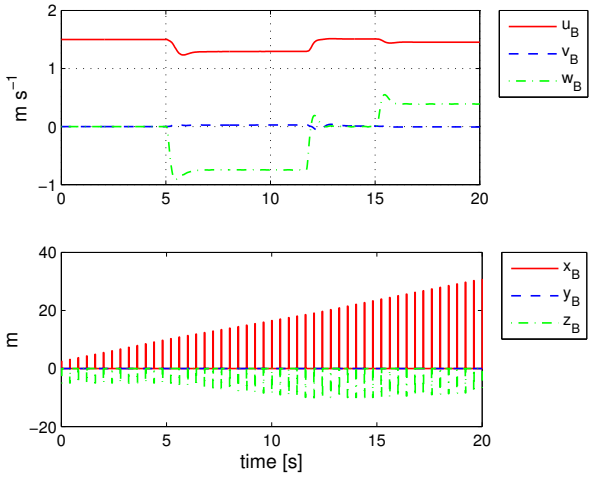

(c) Velocity and Position measurements

Fig. 4. Time evolution of the vehicle variables.

the sampling periods of the other outputs and of the input at $t_s = 0.02$ s.

Table 1. $\mathcal{H}_2$ values vs position sampling rate

Linear position sampling period	0.02	0.04	0.1	0.2	0.4
Closed loop $\mathcal{H}_2$ norm	9.69	9.74	9.90	10.15	10.63

7. CONCLUSIONS

In this paper, the path-following problem for unmanned air vehicles was tackled using an integrated guidance and control approach. The solution consists in reducing the path-following problem to that of regulating an adequately defined error vector to zero. To this end, a gain-scheduling control methodology was presented that takes into account the multi-rate characteristics of the measured outputs. Simulation results showed good performance of the resulting multi-rate integrated guidance and control system in a low altitude terrain following task, when the linear position is available at a rate lower than that of the remaining variables.

REFERENCES

P. Aguiar and J. Hespanha. Trajectory-tracking and path-following of underactuated autonomous vehicles with parametric modeling uncertainty. *IEEE Transactions on Automatic Control*, 52(8):1362–1379, 2007.

D. Antunes, C. Silvestre, and R. Cunha. On the design of multi-rate tracking controllers: An application to rotorcraft guidance and control. In *AIAA Guidance, Navigation, and Control Conference*, SC, 2007. AIAA.

P. Colaneri and G. Nicolao. Multirate lqg control of continuous-time stochastic systems. *Automatica*, 31(4): 591–596, April 1995.

R. Cunha. Modeling and control of an autonomous robotic helicopter. Master's thesis, Instituto Superior Tecnico, Lisbon, Portugal, 2002.

R. Cunha and C. Silvestre. Dynamic modeling and stability analysis of model-scale helicopters with bell-hiller stabilizing bar. In *AIAA Guidance, Navigation, and Control Conference*, TX. AIAA.

R. Cunha and C. Silvestre. A 3D Path-Following Velocity-Tracking Controller for Autonomous Vehicles. In *16th IFAC World Congress*, Praha, Czech Republic, 2005.

I. Kaminer, A. Pascoal, P. Khargonekar, and E. Coleman. A velocity algorithm for the implementation of gain-scheduled controllers. *Automatica*, 31(8):1185–1191, 1995.

S. Lall and G. Dullerud. An lmi solution to the robust synthesis problem for multi-rate sampled-data systems. *Automatica*, 37, 2001.

N. Paulino, C. Silvestre, and R. Cunha. Affine parameter-dependent preview control for rotorcraft terrain following flight. *AIAA Journal of Guidance, Control, and Dynamics*, 29(6):1350–1359, 2006.

W. J. Rugh and J. S. Shamma. Research on gain scheduling. *Automatica*, 36:1401–1425, October 2000.

C. Silvestre, A. Pascoal, and I. Kaminer. On the design of gain-scheduled trajectory tracking controllers. *International Journal of Robust and Nonlinear Control*, 12: 797–839, 2002.

J. Vasconcelos, J. Calvário, P. Oliveira, and C. Silvestre. GPS Aided IMU for Unmanned Air Vehicles. In *Proceedings of the 5th IFAC/EURON Symposium on Intelligent Autonomous Vehicles*, Lisbon, Portugal, July 2004. IST.